

Bio-Nanofluid Flow Through a Stenosed and Porous Arterial Channel Segment with Heating

K.W. Bunonyo¹ and C. Emeruwa²

ABSTRACT

This research focuses on Bio-nanofluid flow through a stenosis and porous arterial channel segment with heating. Blood is taken as the base fluid (base fluid) with the suspension of gold nano-particles, making the solution a biomagnetic and Newtonian nanofluid. We considered mathematical models for the flow of nanofluid and the distribution of heat through the channel past the stenosed segment subject to the moving and no-slip boundary conditions. The models are scaled using some quantities and obtained some dimensionless physical parameters and the governing equations in dimensionless form. Oscillatory perturbation is further applied to reduce the equations to ODE and solved analytical, the constant coefficients are obtained using the boundary conditions in the velocity and temperature profiles. Mathematica codes were developed to simulate the velocity and temperature profiles by varying the resulted physical parameters values within a specific range. Conclusion: It is seen that the velocity and temperature profiles are influence by the radiation parameter, the stenosis height, the length of stenosis, the volume fraction parameter, the Hartmann number, the treatment parameter, Grashof number and the Darcy number, which satisfies the aim of the investigation and is helpful in creating an awareness of the use of nano technology for targeted treatment.

Keywords: Nano-fluid, Stenosis, Heating, Porous, Nanoscience, Viscosity.

MSC 2020 Subject Classification: 35E05, 76D05, 76Z05, 92BC5, 92C35

¹ Department of Mathematics and Statistics, Federal University Otuoke, Nigeria.

² Department of Physics and Electronics, Federal University Otuoke, Nigeria.

1. Introduction

In decades past, the study of nanoscience has expanded in applications in engineering and medical sciences [1]. There are several applications of nanoscience in medical science and bioengineering which reveals that the occlusion of the blood vessels of cancerous tumors, reduction of blood loss during surgeries, development of magnetic devices for cell separation, development of magnetic tracers, targeted transport of drugs using magnetic particles as drug carriers, and cancer tumor treatment causing magnetic hyperthermia [2]. A significant method for cancer therapy is to set a magnetic field close to the cancerous tumor or laser source insight to capture the nano-particles, specifically gold nano-particles, at the tumor site. The gold nano-particles under the influence of the magnetic field or laser beam exhibits the characteristics of a heat source [3]. The temperature of tumor tissues exhibits a characteristic, as clarified in the hypothermia case; when heat is applied from 42°C to 45°C, the cancerous tissue can be distracted. According to Lin et al. [4] in their investigation stated that the duration of cancer therapy can be minimized to half by improving the temperature by 1°C. However, the results of Misra and Shit [5] has made it clear to clinicians and other scientists alike that irreversible damage appears in the blood plasma of patients when the temperature goes above 42°C. At such temperature, a patient rarely survives. The study which involves the injection of nano-particle into the blood veins is referred to as the bio-magnetic fluid dynamic (BFD), whereas, the study which involves the combination of blood and nano-particles is called bio-nanofluid. The bio-nanofluid attains motion due to peristaltic waves produced on the boundaries of blood vessels or the pumping rate of the left ventricle.

In the year 1995, the term nanofluid was elucidated by Choi and Eastman [6] for the first time. Typically, nanofluid is used for advanced heat transfer rate in the base fluid, which is formed by mixing nanometer-sized particles, ranging from 1 to 100 nm, in the conventional base fluid. The commonly used nano-particles are of metals, carbides, oxides, and nano-metals such as graphite and carbon nano-tubes in base fluid. These base fluids include oil, water, alcohol, ethylene glycol, and blood. In recent time, Shah et al. [7] studied nanofluid with magnetic force and thermal trends using numerical and analytical methods. Hsiao [8] researched on nanofluid flow over a stretching surface, with viscous dissipation and magnetohydrodynamic (MHD) effects. Dianchen [9] studied the radiative MHD flow of nanofluid over a non-linear stretching sheet, along with homogeneous/heterogeneous chemical reactions. Zubair et al. [10] investigated a 3D squeezing flow of Darcy Forchimer nanofluid, with the Cattaneo heat model and entropy generation, by considering four different nano-particles. The copper and water nanofluid flow, with a heat source inside a cylindrical annulus, was numerically investigated by Oudina and Bessaïh [11]. Hatami et al. [12] analytically and numerically studied blood–gold nanofluid in a hollow vessel, under consideration of the magnetic field and porous medium. They referred third-grade fluid to blood with gold nano particles and followed the least square method (LSM). Tzirlakis [13] analyzed a 3D fully

developed flow of Newtonian blood flow, with MHD and ferrohydrodynamic, using the finite difference method. Papadopoulos and Tzirtzilakis [14] investigated blood flow based on BFD in a curved square conduit using the SIMPLE method. It is conclusively revealed that the flow could be controlled with an application of an external magnetic field. Misra and Ghosh [15] carried out a research on blood flow in a sheet-like network connected to narrow blood vessels, referred to the lungs through a micro-continuum technique. Misra et al. [16] treated blood as a non-Newtonian fluid and provided a generalized study of blood flow in a magnetic environment and porous medium. Srinivas et al. [17] analyzed the convection characteristics of blood-gold nanofluid in a microchannel with moving and static walls, under the effect of thermal radiation using the homotopy analysis method (HAM).

The above literatures reveal that there is less or no attention given to blood gold-blood nanofluid flow through a stenosed porous arterial segment with heat. This research is to focus on bio-nanofluid flow through a stenosed porous arterial segment with heat, the models follows Bunonyo *et al* [18], with modification to incorporate the nano properties of the fluid and thermal conductivity of the nanofluid, and are solved directly using perturbation method. The solutions are presented graphically for the velocity and temperature profiles respectively.

2. Mathematical Formulation

Let's assume that blood is an unsteady incompressible nanofluid coupled with heat transfer near the walls of a porous and stenosed arterial segment. The fluid is considered to be electrically conducting; as such, an external magnetic field is applied normally to the flow direction. It is assumed that, initially, the system was at rest. However, after a short interval of time, the convection takes place because of the temperature difference, and the fluid starts motion in the x^* - direction and the pumping action of the heart enhances the motion of the fluid. We present the following models governing the flow of nanofluid through a stenosed arterial segment with heat as:

$$\rho_{nf} \frac{\partial w^*}{\partial t^*} = \mu_{nf} \frac{\partial^2 w^*}{\partial y^{*2}} + \rho_{nf} g \beta_T (T^* - T_\infty) - \frac{\mu_{nf}}{k^*} w^* - \sigma B_0^2 w^* \quad (1)$$

$$(\rho c_p)_{nf} \frac{\partial T^*}{\partial t^*} = k_{nf} \frac{\partial^2 T^*}{\partial y^{*2}} - Q_0 (T^* - T_\infty) \quad (2)$$

The corresponding boundary conditions are as:

$$\left. \begin{aligned} \frac{\partial w^*}{\partial y^*} = 0 \quad \frac{\partial T^*}{\partial y^*} = 0 \quad \text{at} \quad y^* = 0 \\ w^* = 0 \quad T^* = T_w \quad \text{at} \quad y^* = R \end{aligned} \right\} \quad (3)$$

The geometry of the stenosis is given as follows:

$$y^*(x) = R_0 - \frac{\delta^*}{2} \left(1 + \cos 2 \frac{\pi x^*}{\lambda} \right) \quad (4)$$

We introduce the following scaling parameters to make the above equations dimensionless:

$$\left. \begin{aligned} x = \frac{x^*}{R_0}; y = \frac{y^*}{R_0}; w = \frac{w^*}{w_\infty}; t = \frac{t^* \nu}{R_0^2}; Gr = \frac{g \beta_T (T_w - T_\infty) R_0^2}{w_\infty \mu_f}; Rd = \frac{Q_0 R_0^2}{(\mu c_p)_f}; \\ \theta = \frac{T^* - T_\infty}{T_w - T_\infty}; \delta^* = \frac{R_0 \delta}{R_T}; Pr = \frac{\mu_{nf} c_{nf}}{k_{nf}}; Ha = B_0 R_0 \sqrt{\frac{\sigma}{\mu_f}}; Da = \frac{k^*}{R_0^2} \end{aligned} \right\}$$

The nano-fluid properties according to Zahir *et al* [19]

$$\left. \begin{aligned} \rho_{nf} = (1 - \phi) \rho_f + \phi \rho_s, (\rho c_p)_{nf} = (1 - \phi) (\rho c_p)_f + \phi (\rho c_p)_s, \\ \frac{k_{nf}}{k_f} = \frac{k_s + 2k_f - 2\phi(k_f - k_s)}{k_s + 2k_f + \phi(k_f - k_s)}, \mu_{nf} = \frac{\mu_f}{(1 - \phi)^{2.5}} \end{aligned} \right\}$$

Using the dimensionless parameters, equation (1) and (2) are reduced to the following:

$$\phi_1 \frac{\partial w}{\partial t} = \frac{\partial^2 w}{\partial y^2} - \left(\frac{1}{Da} \right) w - Ha (1 - \phi)^{2.5} w + Gr_1 \theta \quad (5)$$

$$\phi_2 \frac{\partial \theta}{\partial t} = \frac{1}{Pr} \frac{\partial^2 \theta}{\partial y^2} - Rd\theta \tag{6}$$

where $\phi_1 = \frac{(1-\phi)^{2.5}}{\left((1-\phi) + \phi \frac{\rho_s}{\rho_f} \right)}$; $Gr_1 = \frac{(1-\phi)^{2.5} Gr}{\left((1-\phi) + \phi \frac{\rho_s}{\rho_f} \right)}$; $\phi_2 = \left(1 - \phi + \phi \frac{(\rho c_p)_s}{(\rho c_p)_f} \right)$

The corresponding boundary conditions are as:

$$\left. \begin{aligned} \frac{\partial w}{\partial y} = 0 \quad \frac{\partial \theta}{\partial y} = 0 \quad \text{at} \quad y = 0 \\ w = 0 \quad \theta = 1 \quad \text{at} \quad y = h \end{aligned} \right\} \tag{7}$$

The geometry of the tumor is given as follows:

$$y = 1 - \frac{\delta}{2R_r} \left(1 + \cos 2 \frac{\pi x^*}{\lambda} \right) \tag{8}$$

3. Mathematical Analysis

Considering the pumping rate of the heart, we assume that the solution to equation (5) and (6) can be presented in the following form:

$$\left. \begin{aligned} w &= w_0 e^{i\omega t} \\ \theta &= \theta_0 e^{i\omega t} \\ \chi &= \frac{y}{h} \end{aligned} \right\} \tag{9}$$

Differentiate equation (9) to second order and substitute into equation (5) and (6), we obtained the following:

$$\frac{\partial^2 w_0}{\partial \chi^2} - \beta_1 w_0 = -h Gr_1 \theta_0 \tag{10}$$

$$\frac{\partial^2 \theta_0}{\partial \chi^2} - \beta_2 \theta_0 = 0 \tag{11}$$

where $\beta_1 = h \left(\left(\frac{1}{Da} \right) + Ha(1-\phi)^{2.5} + \phi_1 i \omega \right)$, $\beta_2 = h(Rd + \phi_2 i \omega) Pr$

The corresponding boundary conditions are as:

$$\left. \begin{array}{l} \frac{\partial w_0}{\partial \chi} = 0 \quad \frac{\partial \theta_0}{\partial \chi} = 0 \quad \text{at } \chi = 0 \\ w_0 = 0 \quad \theta_0 = e^{-i\omega t} \quad \text{at } \chi = 1 \end{array} \right\} \quad (12)$$

The geometry of the tumor is given as follows:

$$h = 1 - \frac{\delta}{2R_T} \left(1 + \cos 2 \frac{\pi R_0}{\lambda} x \right) \quad (13)$$

The general solution to equation (11) is given as:

$$\theta_0(\chi) = A \sinh(\sqrt{\beta_2} \chi) + B \cosh(\sqrt{\beta_2} \chi) \quad (14)$$

Solve for the temperature function using the boundary conditions in equation (12) as:

$$\theta_0(\chi) = \left(\frac{e^{-i\omega t}}{\cosh(\sqrt{\beta_2})} \right) \cosh(\sqrt{\beta_2} \chi) \quad (15)$$

Substitute equation (15) into equation (10), we obtain the following:

$$\frac{\partial^2 w_0}{\partial \chi^2} - \beta_1 w_0 = \beta_3 \cosh(\sqrt{\beta_2} \chi) \quad (16)$$

$$\text{where: } \beta_3 = - \left(\frac{Gr_1 e^{-i\omega t}}{\cosh(\sqrt{\beta_2})} \right)$$

The homogenous solution of equation (16) is obtained as:

$$w_0 = A_1 \sinh(\sqrt{\beta_1} \chi) + B_1 \cosh(\sqrt{\beta_1} \chi) \quad (17)$$

The non-homogenous solution of equation (16) is:

$$w_{0p} = \frac{\beta_3}{(\beta_2 - \beta_1)} \cosh(\sqrt{\beta_2} \chi) \quad (18)$$

So that the general solutions will be:

$$w_0 = A_1 \sinh(\sqrt{\beta_1} \chi) + B_1 \cosh(\sqrt{\beta_1} \chi) + \frac{\beta_3}{(\beta_2 - \beta_1)} \cosh(\sqrt{\beta_2} \chi) \quad (19)$$

Applying the boundary condition to solve for the coefficients in equation (19), the solution is as follows:

$$w_0 = \left(\frac{\beta_3}{(\beta_1 - \beta_2)} \frac{\cosh(\sqrt{\beta_2})}{\cosh(\sqrt{\beta_1})} \right) \cosh(\sqrt{\beta_1} \chi) + \frac{\beta_3}{(\beta_2 - \beta_1)} \cosh(\sqrt{\beta_2} \chi) \quad (20)$$

Substitute equation (20) and equation (15) into equation (9), we obtained the following:

$$w = \left(\left(\frac{\beta_3}{(\beta_1 - \beta_2)} \frac{\cosh(\sqrt{\beta_2})}{\cosh(\sqrt{\beta_1})} \right) \cosh(\sqrt{\beta_1} \chi) + \frac{\beta_3}{(\beta_2 - \beta_1)} \cosh(\sqrt{\beta_2} \chi) \right) e^{i\omega t} \quad (21)$$

$$\theta(y) = \left(\frac{1}{\cosh(\sqrt{\beta_2})} \right) \cosh(\sqrt{\beta_2} \chi) \quad (22)$$

4. Presentation of Graphical results

In this section, we carried out numerical simulation of equation (21) and (22) by developing Mathematica code to study the effect of the resulting parameters such as Grashof number, radiation parameter, Hartmann number, Darcy number, the treatment parameter, stenosis growth parameter on the velocity and temperature profiles respectively. In addition, the thermophysical numerical values of blood and gold nano-particles are given in Table1.

**Table1: Numerical values of base fluid and solid material nano-particles
Muhammad *et al.* [20]**

Materials	Base Fluid (Blood)	Nano-particles (Gold)
$\rho(kg / m^3)$	1053	1250
$c_p(J / kgK)$	3594	129
$k(W / mK)$	0.492	318
$\beta_T \times 10^{-5} (K^{-1})$	0.8	1.41
σ	0.18	4.45×10^7
Pr	21	-

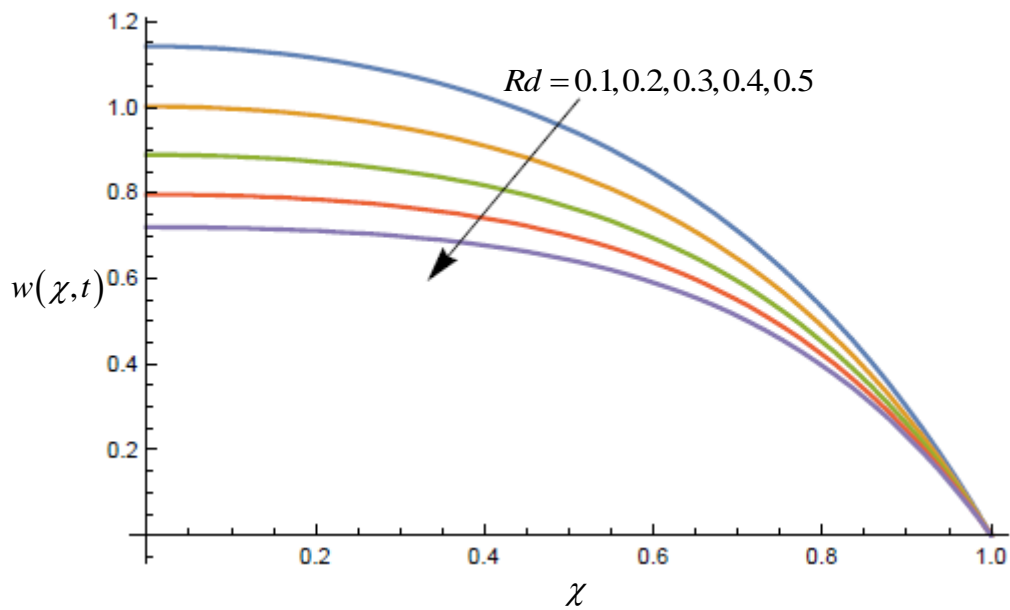


**Figure 1: Influence of Rd values on velocity profile,
when $Pr = 21, Da = 0.05, Gr = 10, Ha = 3, R_T = 0.5, \delta = 0.5$**

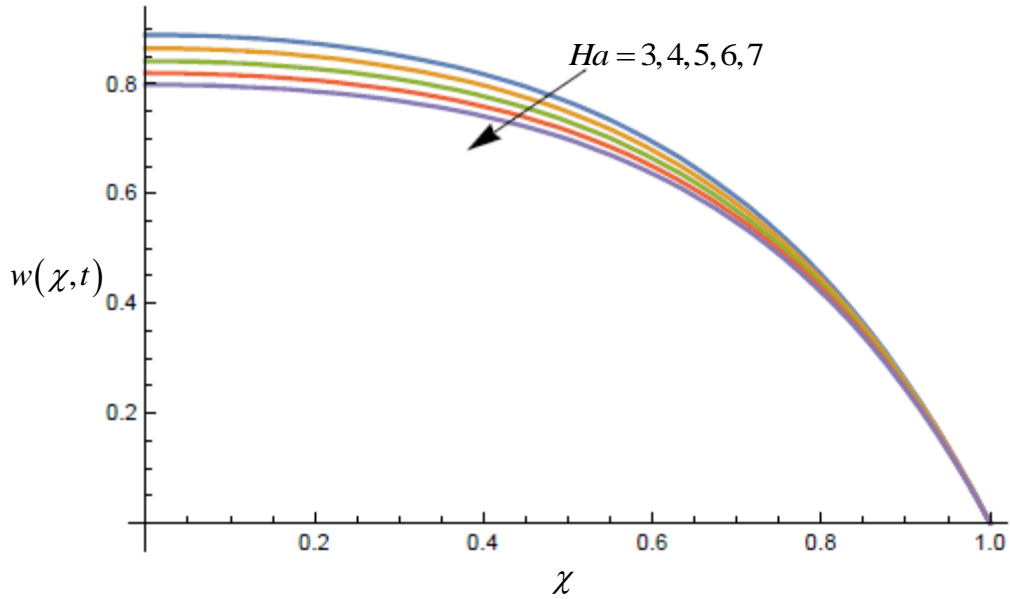


Figure 2: Influence of Ha values on velocity profile,
 when $Pr = 21, Da = 0.05, Gr = 10, \delta = 0.5, R_T = 0.5, Rd = 0.3, \phi = 0.04, \lambda = 2$

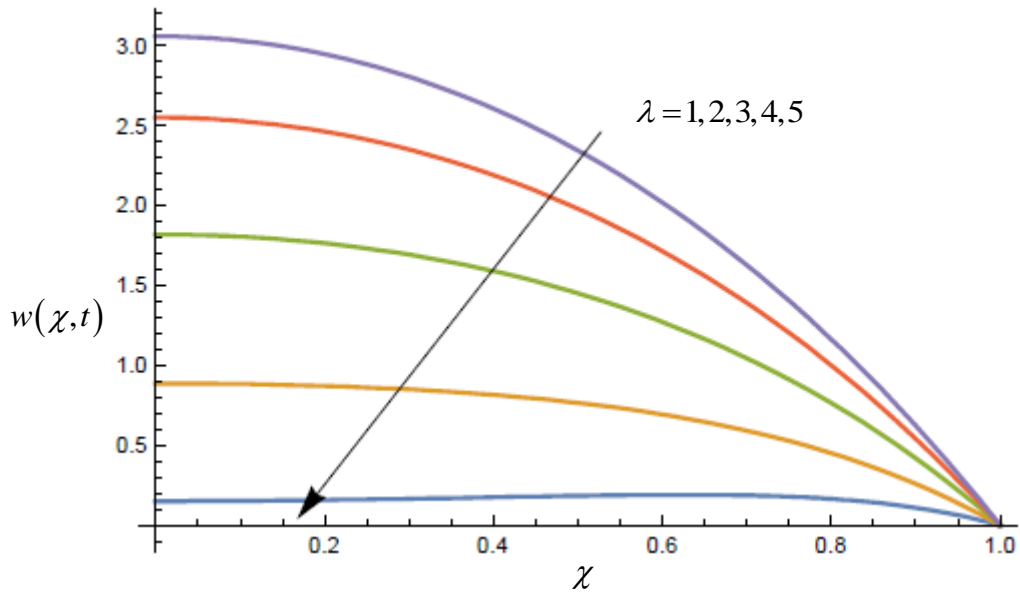


Figure 3: Influence of λ values on velocity profile,
 when $Pr = 21, Da = 0.05, Gr = 10, Ha = 3, R_T = 0.5, Rd = 0.3, \delta = 0.5, \phi = 0.04$

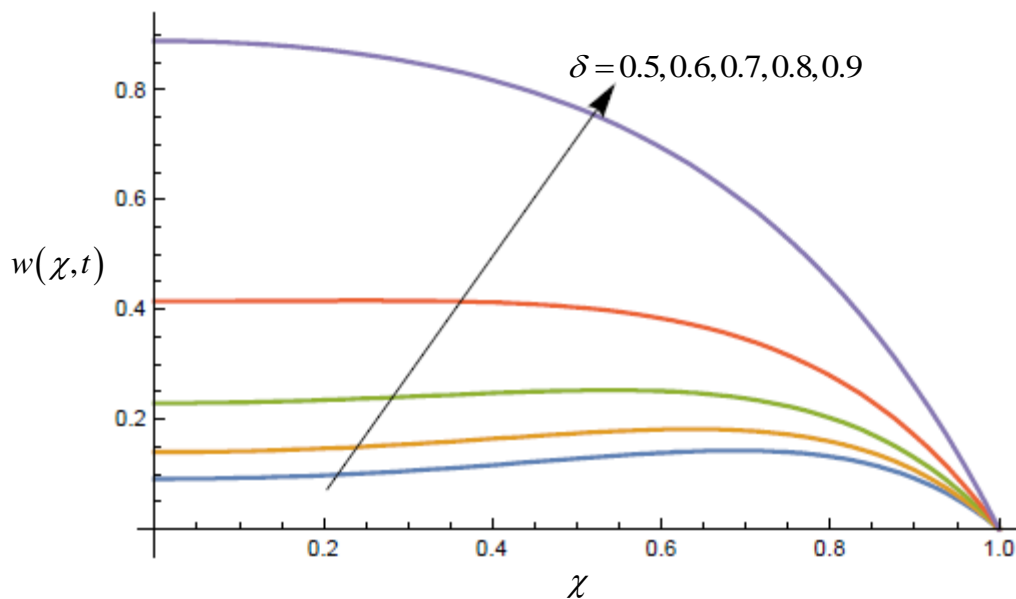


Figure 4: Influence of δ values on velocity profile,
when $Pr = 21, Da = 0.05, Gr = 10, Ha = 3, R_T = 0.5, Rd = 0.3, \lambda = 2, \phi = 0.04$

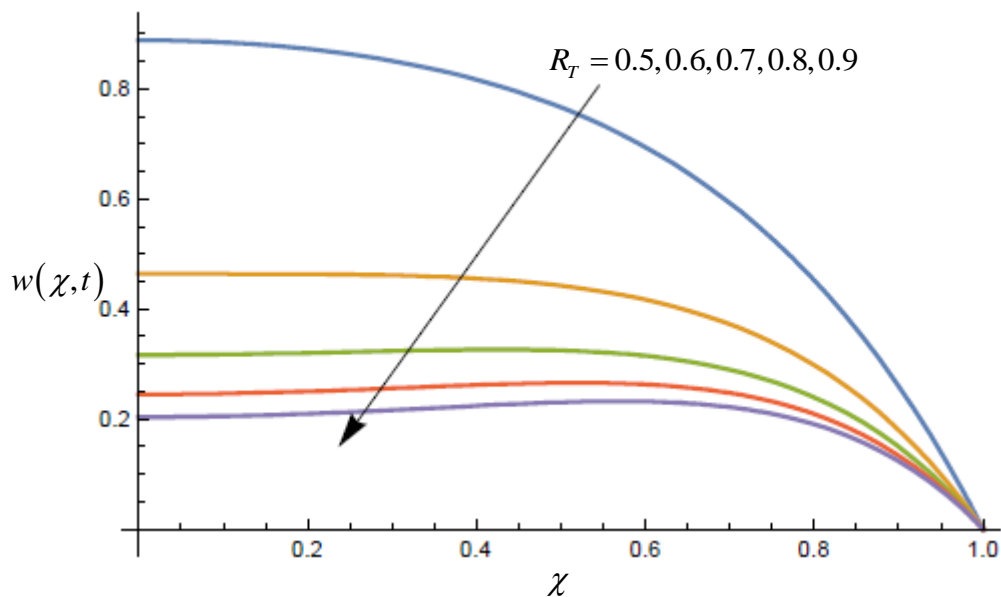


Figure 5: Influence of R_T values on velocity profile,
when $Pr = 21, Da = 0.05, Gr = 10, Ha = 3, \delta = 0.5, Rd = 0.3, \lambda = 2, \phi = 0.04$

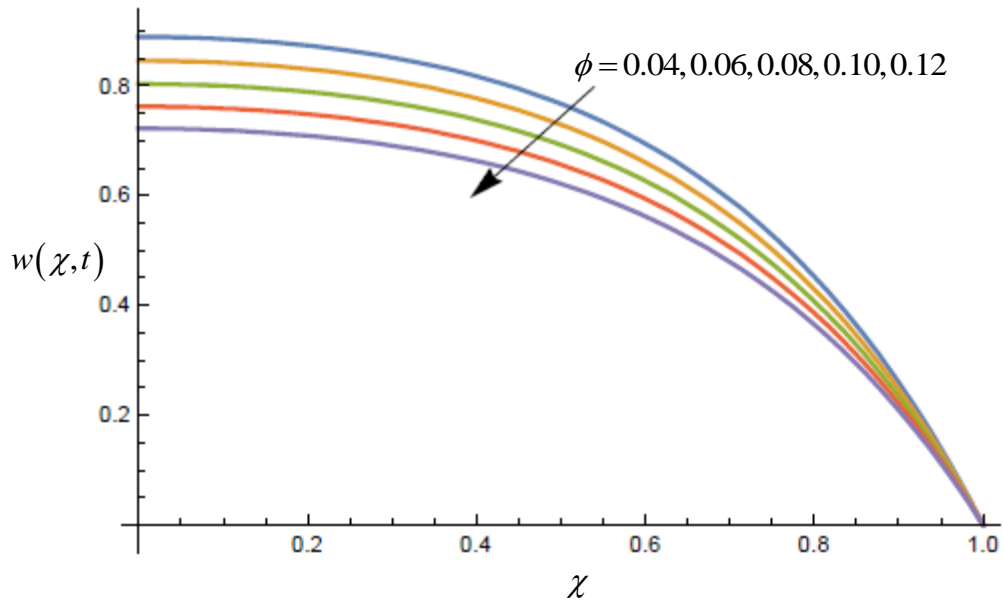


Figure 6: Influence of ϕ values on velocity profile,
when $Pr = 21, Da = 0.05, Gr = 10, Ha = 3, R_T = 0.5, Rd = 0.3, \delta = 0.5, \lambda = 2$

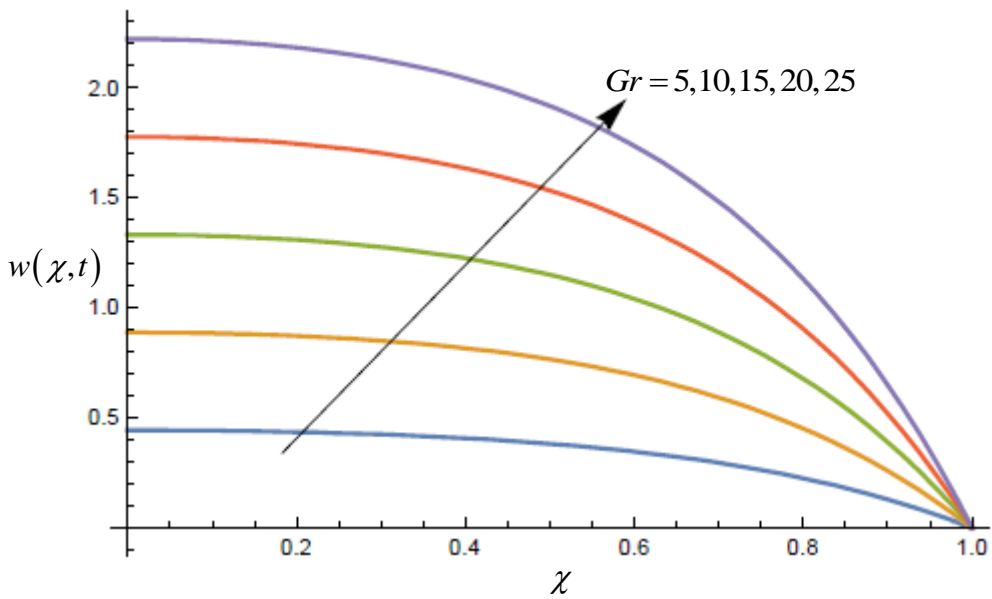


Figure 7: Influence of Gr values on velocity profile,
when $Pr = 21, Da = 0.05, \delta = 0.5, Ha = 3, R_T = 0.5, Rd = 0.3, \phi = 0.04, \lambda = 2$

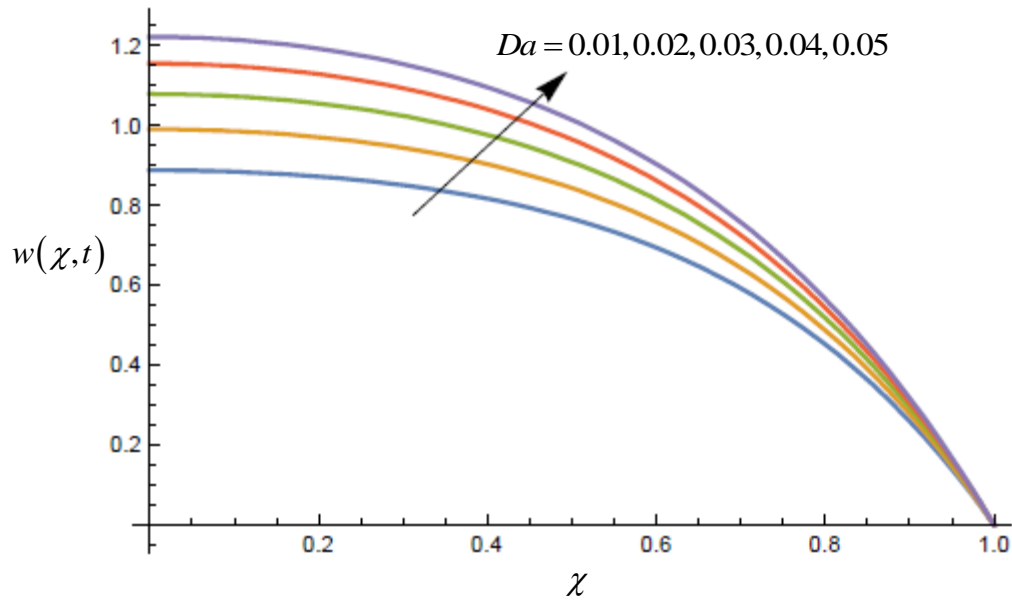


Figure 8: Influence of Da values on velocity profile,
when $Pr = 21, \delta = 0.5, Gr = 10, Ha = 3, R_T = 0.5, Rd = 0.3, \phi = 0.04, \lambda = 2$

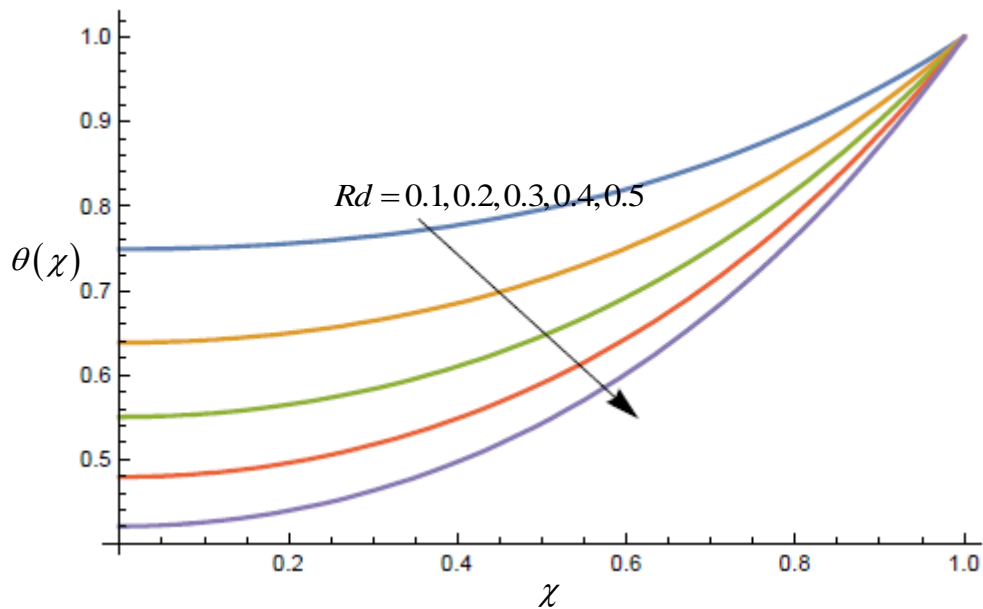


Figure 9: Influence of Rd values on temperature profile,
when $Pr = 21, \delta = 0.5, R_T = 0.5, \phi = 0.04, \lambda = 2$

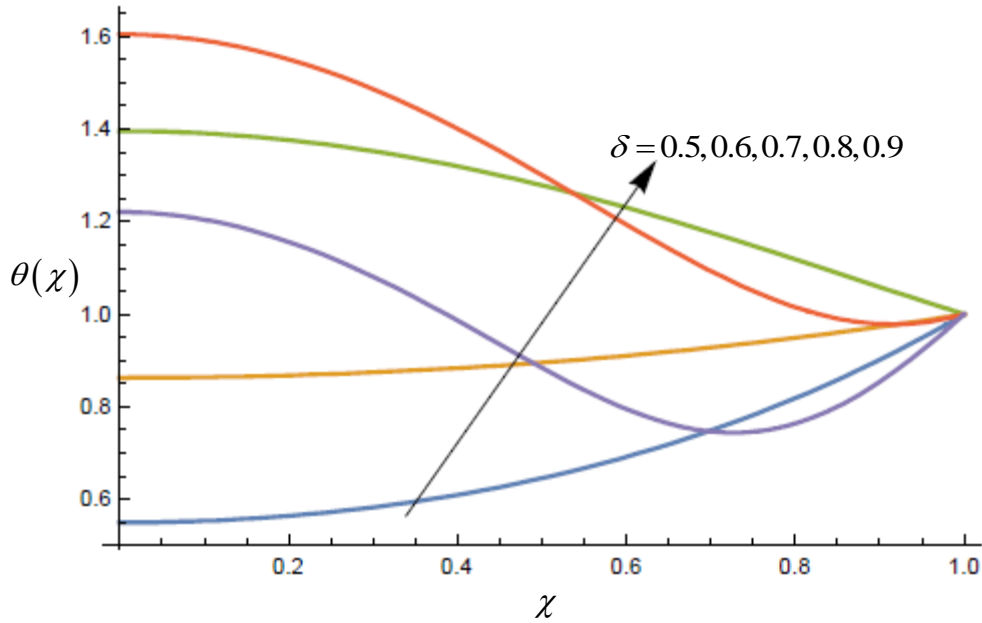


Figure 10: Influence of δ values on temperature profile, when $Pr = 21, Rd = 0.3, R_r = 0.5, \phi = 0.04, \lambda = 2$

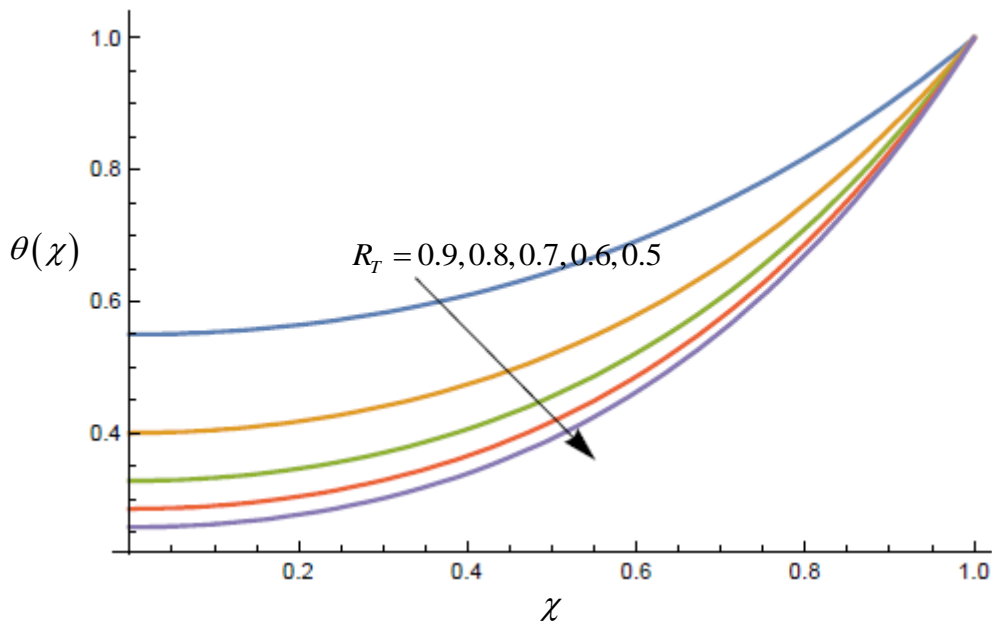


Figure 11: Influence of R_r values on temperature profile, when $Pr = 21, \delta = 0.5, Rd = 0.3, \phi = 0.04, \lambda = 2$

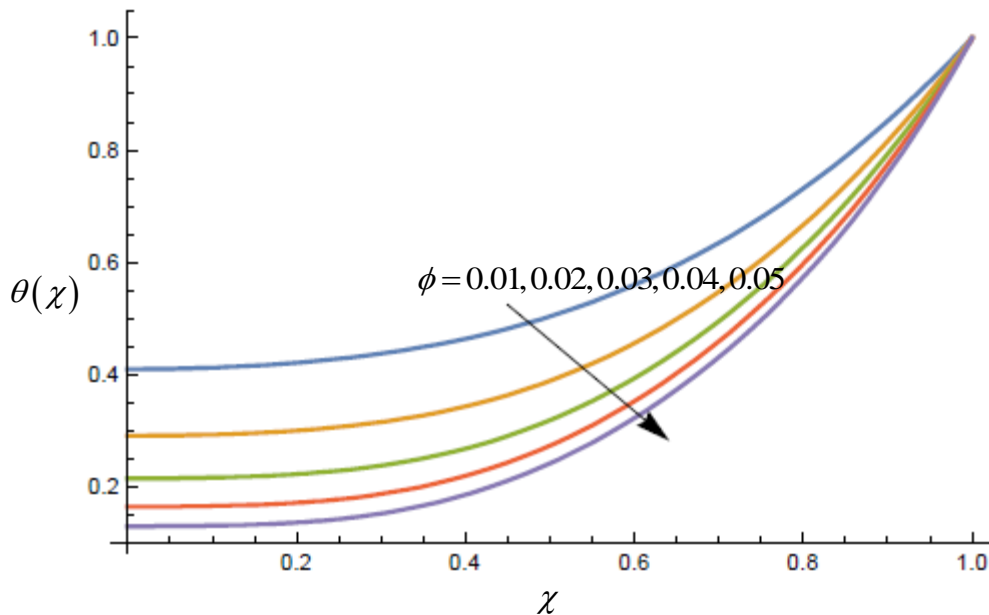


Figure 12: Influence of ϕ values on temperature profile, when $Pr = 21, \delta = 0.5, R_T = 0.5, Rd = 0.3, \lambda = 2$

5. Discussion of Graphical results

The numerical simulation has been carried out by using the following parameters values within a range of haemodynamical flows: $Rd = 0.3, R_T = 0.5, \delta = 0.5, Da = 0.05, Pr = 21, Ha = 3, x = 0.3, Gr = 10, \phi = 0.04, \omega = 0.3, t = 5, \lambda = 2$ to validate our model.

Figure 1 illustrates that increase in the radiation parameter values, decreases the velocity profile of the fluid. The figures goes further to tell that at the centre line of the channel the velocity profile increase but decelerates as the boundary layer increases. The influence of the Hartmann number is seen in **Figure 2**. This figure shows that the velocity profile decreases as the Hartmann number increase, and this is due to the fact that if a magnetic is applied perpendicular to a moving fluid such as blood, it generates a force called Lorentz force, which opposes the motion. In **Figure 3** result shows the influence of the length of stenosis on the velocity profile. The figure depicts that the length of stenosis increase caused a decrease in the velocity profile of the fluid flow with other pertinent parameters values playing key roles. **Figure 4** illustrates the increase in velocity profile, for a decrease in the height of stenosis. It means that the height of stenosis is been taken care of with the presence of the treatment such as statin in the bloodstream. The influence of the treatment parameter is seen in **Figure 5**, the figure clear show the decrease in velocity profile with an increase of treatment parameter values. This decrease depicts an application of ineffective treatment could lead to a decrease in the

velocity profile. The fraction concentration parameter values increase affects the velocity profile to decreases as seen in **Figure 6**. **Figure 7** shows velocity profile increase with the increase in Grashof number. This velocity profile increases indicates that there is greater viscous force over thermal viscous in the fluid. **Figure 8** depicts that the velocity profile increases with the increase in Darcy number. This shows that as the region becomes porous, the more the velocity of the fluid flowing through that region.

The temperature profile is shown with **Figure 9 – Figure 12**. In **Figure 9** the temperature profile increases with the increase in radiation. This is of the fact that the radiation heat up the region and enhance blood flow. The velocity profile increases with the increase of height of stenosis; this temperature increase is the fact that the treatment parameter has taking care of the height and it enhances the temperature distribution as illustrated in **Figure 10**.

Figure 11 illustrates the decrease in temperature distribution with an increase of the treatment parameter values. This result is of the view that treatment parameter opposes temperature distribution. Finally, **Figure 12** depicts the decrease of temperature profile with the increase of the fraction concentration values.

6. Conclusion

Having carried out the formulation of the models, solving the governing equations using oscillatory perturbation method and numerical simulation was done using Mathematica 10, we conclude as follows:

1. The velocity profile increases with the increase in Grashof number, the height of stenosis and Darcy parameter.
2. The velocity profile decreases with an increase in radiation parameter, Hartmann number, length of stenosis, treatment parameter and the fraction concentration parameter.
3. The temperature profile increases with an increase of the radiation parameter and the height of stenosis.
4. The temperature profile decreases with an increase of the treatment parameter and the fraction concentration parameter.

References

- [1] Franconi, C. Hyperthermia heating technology and devices. In *Physics and Technology of Hyperthermia*; Springer: Berlin/Heidelberg, Germany, 1987; pp. 80–122.
- [2] Saqib, M.; Khan, I.; Shafie, S. Generalized magnetic blood flow in a cylindrical tube with magnetite dusty particles. *J. Magn. Magn. Mater.* 2019, 484, 490–496.
- [3] Ebaid, A.; Aljohani, A.F.; Aly, E.H. Homotopy perturbation method for peristaltic motion of gold-blood nanofluid with heat source. *Int. J. Numer. Methods Heat Fluid Flow* 2019, 30, 3121–3138.
- [4] Lin, W.L.; Yen, J.Y.; Chen, Y.Y.; Jin, K.W.; Shieh, M.J. Relationship between acoustic aperture size and tumor conditions for external ultrasound hyperthermia. *Med Phys.* 1999, 26, 818–824.
- [5] Misra, J.; Shit, G. Biomagnetic viscoelastic fluid flow over a stretching sheet. *Appl. Math. Comput.* 2009, 210, 350–361.
- [6] Choi, S.U.; Eastman, J.A. *Enhancing Thermal Conductivity of Fluids with Nanoparticles*; Argonne National Lab.: Lemont, IL, USA, 1995; pp. 99–105.
- [7] Shah, Z.; Islam, S.; Ayaz, H.; Khan, S. Radiative heat and mass transfer analysis of micropolar nanofluid flow of Casson fluid between two rotating parallel plates with effects of Hall current. *J. Heat Transf.* 2019, 141, 022401.
- [8] Hsiao, K.-L. Micropolar nanofluid flow with MHD and viscous dissipation effects towards a stretching sheet with multimedia feature. *Int. J. Heat Mass Transf.* 2017, 112, 983–990.
- [9] Lu, D.; Ramzan, M.; Ahmad, S.; Chung, J.D.; Farooq, U. A numerical treatment of MHD radiative flow of Micropolar nanofluid with homogeneous-heterogeneous reactions past a nonlinear stretched surface. *Sci. Rep.* 2018, 8, 1–17.
- [10] Zubair, M.; Shah, Z.; Islam, S.; Khan, W.; Dawar, A. Study of Three dimensional Darcy–Forchheimer squeezing nanofluid flow with Cattaneo–Christov heat flux based on four different types of nanoparticles through entropy generation analysis. *Adv. Mech. Eng.* 2019, 11, 1687814019851308.
- [11] Mebarek-Oudina, F.; Bessaïh, R. Numerical simulation of natural convection heat transfer of copper-water nanofluid in a vertical cylindrical annulus with heat sources. *Thermophys. Aeromechanics* 2019, 26, 325–334.
- [12] Hatami, M.; Hatami, J.; Ganji, D.D. Computer simulation of MHD blood conveying gold nanoparticles as a third grade non-Newtonian nanofluid in a hollow porous vessel. *Comput. Methods Programs Biomed.* 2014, 113, 632–641.
- [13] Tzirtzilakis, E. A mathematical model for blood flow in magnetic field. *Phys. Fluids* 2005, 17, 077103.
- [14] Papadopoulos, P.; Tzirtzilakis, E. Biomagnetic flow in a curved square duct under the influence of an applied magnetic field. *Phys. Fluids* 2004, 16, 2952–2962.

- [15] Misra, J.; Ghosh, S. A mathematical model for the study of blood flow through a channel with permeable walls. *Acta Mech.* 1997, 122, 137–153.
- [16] Misra, J.; Sinha, A.; Shit, G. A numerical model for the magnetohydrodynamic flow of blood in a porous channel. *J. Mech. Med. Biol.* 2011, 11, 547–562.
- [17] Srinivas, S.; Vijayalakshmi, A.; Reddy, A.S. Flow and heat transfer of gold-blood nanofluid in a porous channel with moving/stationary walls. *J. Mech.* 2017, 33, 395–404.
- [18] Bunonyo, KW, Emeka Amos. Lipid Concentration Effect on Blood
- [19] Flow Through an Inclined Arterial Channel with Magnetic Field. *Mathematical Modelling and Applications*. Vol. 5, No. 3, 2020, pp. 129-137. doi: 10.11648/j.mma.20200503.11
- [20] Shah, Z., Khan, A., Khan, W., Alam, M. K., Islam, S., Kumam, P., & Thounthong, P. (2020). Micropolar gold blood nanofluid flow and radiative heat transfer between permeable channels. *Computer Methods and Programs in Biomedicine*, 186, 105197.
- [21] Saqib, M., Khan, I., Chu, Y. M., Qushairi, A., Shafie, S., & Nisar, K. S. (2020). Multiple Fractional Solutions for Magnetic Bio-Nanofluid using Oldroyd-B Model in a Porous Medium with Ramped Wall Heating and Variable Velocity. *Applied Sciences*, 10(11), 3886.

Nomenclature

w^*	Dimensional velocity profile
w_0	Perturbed velocity profile
x^*, y^*	Dimensional distances
R	Radius of an abnormal arterial segment
R_0	Radius of normal artery
R_T	Treatment parameter
Ha	Hartmann number
δ	Stenosis height
Rd	Radiation parameter
k_{nf}	Thermal conductivity of nano-fluid
k_f	Thermal conductivity of base fluid (blood)
Da	Darcy number
Gr	Thermal Grashof number
β_T	Volumetric expansion
ϕ	Volumetric fraction concentration
B_o	Strength of applied magnetic field
c_p	Specific heat capacity at constant pressure
Pr	Prandtl number for blood
T^*	Temperature of blood
T_∞^*	Far field temperature

Greek Symbols

ν	Kinematic viscosity of blood
μ_{nf}	Dynamic viscosity of nano-fluid
μ_f	Dynamic viscosity of base fluid (blood)
g	Acceleration due to gravity
λ	Length of stenosis
ω	Oscillatory frequency
θ	Dimensionless temperature
θ_o	Dimensionless perturbed temperature
ρ_s	Density of the solid nano-particle
ρ_f	Density of the base fluid